https://doi.org/10.2352/ISSN.2169-4451.2019.36.1

Fabrication of Magnetic Polymer Nanocomposites Using Inkjet 3D Print Technology

Madeleine Cannamela[1,2]; Jim Stasiak[3]; Paul Harmon[4]; Thomas Allen[4]; Pallavi Dhagat[1]; 1. Oregon State University, Corvallis, OR, USA; 2. HP Inc.; Corvallis, OR, USA; 3. HP Labs; Corvallis, OR, USA; 4. Nanovox, LLC; Corvallis, OR, USA

Abstract

Tailored magnetic nanocomposites have applications ranging from communications technologies to medical devices. Using a novel 3D fabrication technique that combines thermal inkjet and powder bed fusion print technologies, magnetic composites were fabricated by jetting magnetic nanoparticle containing ink into a polymer powder bed and then heat fusing the ink/polymer matrix. The goals were to demonstrate the feasibility of nanocomposite fabrication with controllable magnetic properties by varying the volume fraction of magnetic ink jetted into the polymer as well as to experimentally validate the effective medium theory based model developed to predict the permeability of the composites as a function of its magnetic particle concentration. As expected, magnetic susceptibility and saturation magnetization were seen to increase with the volume fraction of magnetic particles in the composites.

Introduction

Additive manufacturing technologies offer the ability to create novel structures and functional materials by design [1]. Composites produced by a mixture of polymers and nanoparticles represent an important class of engineered materials that have been the subject of both academic and industrial investigations for the last few decades. Many of these engineered materials exhibit enhanced mechanical [2], electrical [3], thermal, optical [4] [5], and magnetic [6] properties compared with standard bulk materials. In this work, magnetic polymer nanocomposites were prepared using an additive manufacturing technology that combines aspects of polymer bed fusion and inkjet materials jetting [7] to enable voxel-scale (1200 dots per linear inch by 80 µm thick) [8] tailoring of magnetic properties. A thermal inkjet printhead containing ink with dispersed ferrite nanoparticles enabled drop-on-demand depositions into a polymer powder bed. Magnetic nanocomposites have applications including in RF lenses [6], communications technologies [9], soft robotics [10] [11] and medical devices [12]. Current fabrication techniques include fiber (or filament) deposition modeling [10] [11] [13], inkjet printing onto solid substrates [9], screen printing of magnetic nanoparticle pastes [14] and melt blending of polymers and nanoparticles [12]. Filament printing is limited in its ability to adjust nanoparticle concentration during printing unless multiple filaments are used. Inkjet printing onto a solid substrate allows spatial control over the magnetic material being added but can only create films not 3D structures. The last two techniques allow no ability to selectively vary nanoparticle concentration throughout the composite. The combination of polymer bed fusion and materials jetting allows the creation of complex structures in 3D and precisely varied functionality.

For this study, magnetic properties were tailored by varying the volume fraction of magnetic nanoparticles in different composite samples. Saturation magnetization and magnetic susceptibility were measured for each composite to determine trends between volume fraction and magnetic properties. Future work will include fitting a mathematical model to the measured magnetic susceptibility data. Composite magnetic properties do not follow models for bulk magnetic materials [15] [16]. Instead, a model based on effective medium theory (EMT) is needed to account for the magnetic behavior of composites that contain magnetic and non-magnetic materials. This model should allow magnetic properties to be predicted for any volume fraction, enabling the selection of magnetic properties throughout a 3D print as precisely as colors in a 2D print.

Ultimately magnetic susceptibility modeling will be combined with past research and EMT modeling for printed dielectric materials [6], enabling printing of voxel tailored composites with magnetic and dielectric properties.

Materials and Processes

Development of ink

Custom nickel zinc ferrous oxide nanoparticles (30 nm mean diameter) are functionalized with surface ligands for dispersion in a thermal inkjet compatible fluid of 7 cP viscosity and 45 mN/m surface tension. The details of particle composition and functionalization are proprietary. The ink is prepared by Nanovox, LLC. This ink is then loaded into a thermal inkjet printhead.

Fabrication of samples with varied magnetic nanoparticle volume fraction

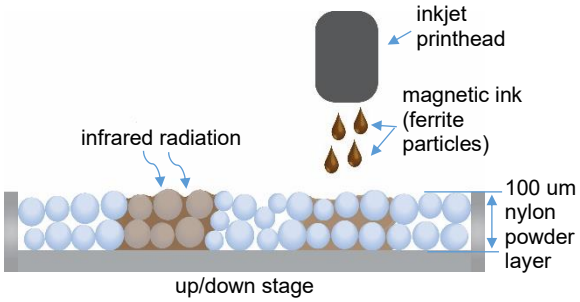

Figure 1. *Illustration of the printing process. Magnetic ink, in programmable volumes within a voxel, followed by a heat-absorbing ink is deposited in a ~100 µm thick polymer (nylon PA12) powder layer. Infrared radiation results in the polymer/particle matrix being fused into a composite material.*

The nanocomposites were printed using an experimental 3D printer built to mimic commercially available powder bed fusion and materials jetting combination printers [8]. Figure 1 shows a schematic of the print process. First, the heat-fusible nylon powder was spread by hand with a metal blade across a heated

stage held at 174 °C (i.e. a few degrees below melt of the nylon polymer). The stage height was adjusted by a micrometer to control the thickness of the powder layer (~100 µm). Next, the magnetic ink was jetted from the printhead into the powder. Printhead parameters including drop frequency, drop placement, number of drops per voxel and number of times an area was printed (known as print passes) were controlled by software. The magnetic nanoparticles were carried into the powder by the ink fluid and retained on the polymer particles in a process known as voxel doping. Physiochemical interactions between the functionalized nanoparticles and polymer powder govern the rate, density and distribution of nanoparticles throughout the polymer matrix [17]. Finally, heat-absorbing ink was printed into the composite matrix to enable fusing of the polymer powder upon exposure to infrared radiation. The powder spread, infiltration and fusing process was repeated until printed samples robust enough for handling (~500 µm thick) were obtained.

Results and Discussion

Physical properties characterization of samples

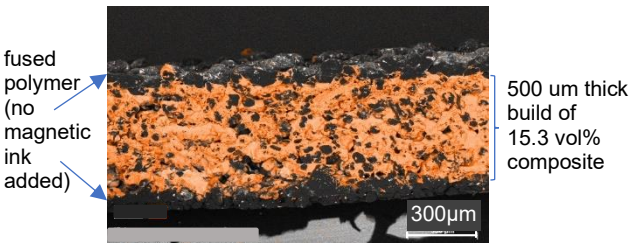

Figure 2. *SEM/EDS map of printed composite with uniformly distributed magnetic nanoparticles (orange).*

Figure 2 shows a scanning electron microscopy/energy dispersive X-ray spectroscopy (SEM/EDS) image of a cross-sectioned magnetic nanocomposite sample. The ferrite-rich areas are highlighted in orange. Each sample consisted of 5 doped layers with additional undoped top and bottom layers to allow for sample handling (undoped layers are not considered in sample build thickness). EDS confirms that magnetic particles are homogeneously distributed in the fabricated composites. SEM offers a qualitative view of polymer packing density and voiding in samples which affect structural integrity.

Figure 3 shows thermogravimetric analysis (TGA) results for nanocomposites printed with varying volume fractions of magnetic nanoparticles. TGA showed our samples ranged from 2.2 vol% to 15.3 vol% of magnetic nanoparticles. To calculate the nanoparticle volume percent in each composite, TGA measured masses and densities published for each component in literature were used. Density used for the nickel zinc ferrous oxide nanoparticles was 5.18 g/cm^3 [18], [19] and for the polymer was 1.03 g/cm^3 [20]. Samples of a known area were punched from the printed composites and pyrolyzed under nitrogen gas to 700 °C leaving a mix of magnetic nanoparticles and organic residue from the polymer. A control sample, containing no magnetic particles, was analyzed to calibrate the mass of residue per gram of polymer. This amount was subtracted from the magnetically doped samples to determine the final magnetic particle content.

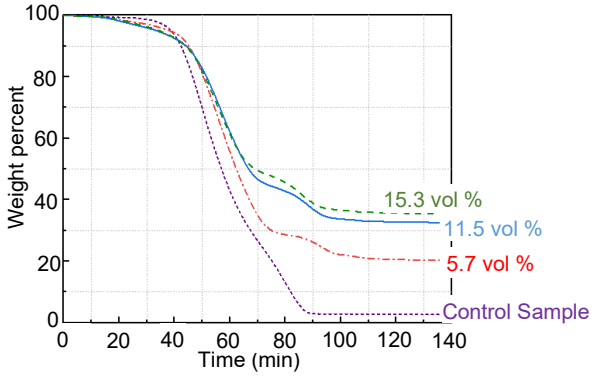

Figure 3. *TGA of composite samples. Final magnetic nanoparticle weights were obtained after subtracting the residual weight of the control sample.*

As seen from Table 1, the mass of nanoparticles in the composite increases nearly proportionally with number of passes. Additionally, TGA of different samples with equal number of print passes showed that ink can be dispensed accurately and repeatably from the inkjet printhead based on the percent standard deviations, all less than 10% (Table 1, column 2). By comparison, the amount of polymer varies widely from sample to sample (Table 1 column 3), indicating inconsistent thickness control of the polymer layers. A more precisely adjustable stage and automated control of spreading should mitigate this variability. Data are shown for 2 samples of 4 passes and 12 passes, and 3 samples of 8 passes. Future work will include additional replicates to improve statistical accuracy.

Table 1: Variation of nanoparticle mass and polymer mass

Number of Print Passes of Magnetic Ink	Average Mass of Nanoparticles (mg)	Average Mass of Polymer (mg)
4 Pass	2.5± 0.1%	24.5± 23%
8 Pass	4.6± 1.5%	32.3± 6.6%
12 Pass	6.9± 3.7%	29.5± 31%

Magnetic properties characterization of samples

Saturation magnetization and susceptibility (normalized for sample volume) were measured for each sample. Saturation magnetization was determined by a room temperature vibrating sample magnetometer and susceptibility by a physical properties measurement system (from Quantum Design, Inc.) used in the alternating current susceptibility mode [21]. Magnetic properties as a function of volume fraction can be seen in Figures 4 and 5.

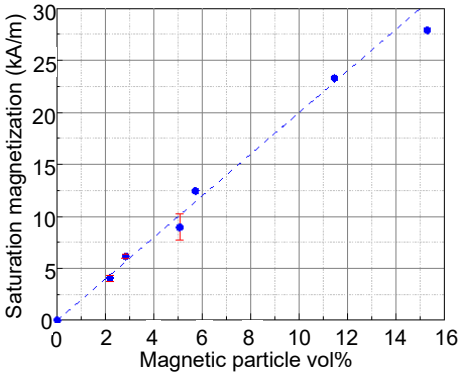

Figure 4. *The saturation magnetization is obtained by normalizing the measured saturation moment with the sample volume. The error bars are attributed to the imprecise control of the powder layer thickness which lead to variation in the sample volume.*

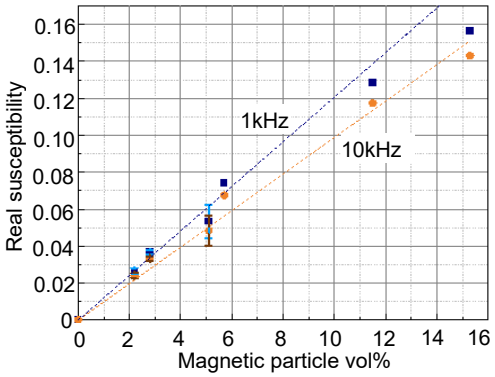

Figure 5. *Susceptibility as a function of the magnetic particle volume percentage in the samples with a linear fit.*

As expected, both saturation magnetization and susceptibility increase with the volume fraction of magnetic particles in the composite. A maximum saturation magnetization of ~28 kA/m was measured at 15.3 vol%. It is anticipated that volume fractions as high as 40 vol% may be achieved while maintaining structural integrity. Linear extrapolation predicts a saturation magnetization of 75 kA/m for a 40 vol% nanocomposite. For comparison, the saturation magnetization of bulk ferrite materials, depending on their composition, ranges between 240 kA/m and 480 kA/m [22]. Adjusting the stoichiometry of the ferrite nanoparticles could allow higher maximum magnetic properties in the composites [23]–[25] than the current formulation.

Modeling and Analysis Using the Effective Medium Theory

An objective of this work is to develop 3D printing processes that enable the fabrication of novel materials using inkjet-based 3D printing technologies. For these fabrication processes to be technologically useful, they must be both predictable and reproducible. Specifically, the development of predictive models that provide quantitative information about the nanoparticle volume fraction and the desired physical properties of the composite are required. For magnetodielectric polymer nanocomposite materials, properties that influence electromagnetic response to high-frequency signals include the effective electrical conductivity, σ_{eff}, effective dielectric permittivity, ε_{eff}, and the effective magnetic permeability, μ_{eff}. The determination of these three parameters is required to calculate the effective complex electromagnetic wave impedance of the composite material Z_{eff}:

$$Z_{eff} = \sqrt{(j\omega\mu_{eff}/(\sigma_{eff} + j\omega\varepsilon_{eff}))} \quad (1)$$

where ω is the electromagnetic wave frequency, and j is the imaginary unit. Each of these effective material properties is dependent on the volume fraction (number density) of the magnetodielectric nanoparticles embedded in the polymer medium. For many polymer nanocomposites, analysis and predictive modeling can be done within the framework of the Effective Medium Theory (EMT). While the use of EMT methods to analyze and model the magnetic properties of ferrite-loaded polymer nanocomposites has been successful, a thorough discussion of this topic is outside of the scope of this paper. However, most often, these methods have been applied to two-component composite systems consisting of a polymer medium and homogeneously embedded nanoparticles. An important observation has been that the fused composite samples always had some degree of porosity based on cross-sectional imaging and TGA of the samples produced for this study. That is, in addition to the embedded nanoparticles, the samples contained microscopic air voids distributed homogeneously through the fused composite layer. A consequence arising from the embedded voids is that both the nanoparticles and the voids contribute to the dielectric permittivity of the fused samples. The coexistence of nanoparticles and microscopic air voids in the composite layer suggests that modeling using two-component EMT mixing formulas may not be accurate. Instead, a three-component EMT model is required to predict the effective properties of fused, microporous polymer nanocomposites. As part of this study, a new approach for modeling composite materials with multiple dielectric inclusions was developed. The approach involves an iterative technique that systematically reduces the multi-component system to a simple two-component system making it possible to use traditional EMT mixing formulas. Validation of the model using the magnetodielectric polymer nanocomposites discussed in this paper are currently underway. Once validated, the details describing the model and a comparison to measured results will be discussed in a future publication. However, to illustrate the use of the technique, the evaluation of a polymer nanocomposite consisting of a polymer matrix, dielectric nanoparticles, and microscopic air voids is provided (figure 6).

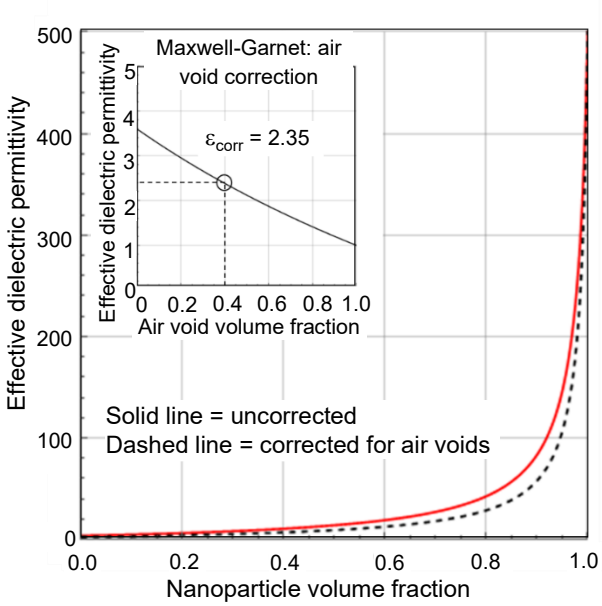

Figure 6*. A three-component dielectric polymer composite consisting of a polymer matrix, dielectric nanoparticles and microscopic air voids evaluated using the iterative EMT model.*

The effect of microscopic air voids on the effective dielectric permittivity of a polymer nanocomposite is shown in Figure 6. In the example, reference values for the relative dielectric permittivity of polyamide 12 (PA12) (ε_r = 3.6) and $BaTiO_3$ nanoparticles (ε_r = 500) are used as model parameters for the polymer nanocomposite. In the example, the first step of the procedure is to calculate the effective dielectric permittivity of a composite consisting of only polymer and air voids using the Maxwell-Garnett (MG) mixing formula,

$$\varepsilon_{eff} = \varepsilon_e + 3\phi\varepsilon_e((\varepsilon_i-\varepsilon_e)/(\varepsilon_i+2\varepsilon_e-\phi(\varepsilon_i-\varepsilon_e))) \quad (2)$$

where ε_{eff}, ε_i and ε_e are the effective dielectric permittivity, nanoparticle relative permittivity, and polymer medium relative permittivity respectively, and ϕ is the volume fraction of the inclusions [26]. The dielectric permittivity of air is set to $\varepsilon_{air} = 1.0$. In the Fig. 6 inset, the dependence of the effective dielectric permittivity on the volume fraction of the microscopic, spherical air voids is shown. Note that since the relative dielectric permittivity of the PA12 is larger than that of the air voids, the dependence has a negative slope. Next, in this example, the effective dielectric permittivity of a composite consisting of PA12 and $BaTiO_3$ nanoparticles is calculated using Eq. 2 assuming a composite to be void-free and represented by the solid line in Fig. 6. Finally, the calculation is repeated using the adjusted dielectric permittivity of the PA12/air void composite for a specific air void volume fraction. In the example, the air void volume fraction is assumed to be 0.4. Using the curve shown in the inset, an air volume fraction of $\phi = 0.4$ yields a new, *reduced* relative dielectric permittivity for the medium of $\varepsilon_{corr} = 2.35$. The dashed line in Fig. 6 shows the effect of the reduced relative dielectric permittivity of the medium on the overall effective dielectric permittivity for a composite of polymer, dielectric nanoparticles, *and* air voids. The three-component EMT model developed in this study provides a convenient method to include porosity in the calculation of the effective dielectric permittivity for 3D-printed polymer nanocomposites. Note that the method provides an estimate and not a rigorous result obtained using formal effective medium theory.

While the effect of including air voids in this example is small, it is not negligible. For example, using the adjusted effective dielectric permittivity, $\varepsilon_{eff,}$ becomes an important factor when designing a magnetodielectric polymer nanocomposite material for an application that requires a specific effective electromagnetic wave impedance. While the presence of air voids in a magnetodielectric polymer nanocomposite will have little effect on the effective magnetic permeability, μ_{eff}, the presence of voids directly affects the effective dielectric permittivity. Recall that the effective electromagnetic wave impedance, $Z_{eff,}$ is a function of both μ_{eff} and $\varepsilon_{eff,}$ as shown in Eq.1.

As discussed in the introduction, the objective of this research is to fabricate magnetodielectric materials and devices using an inkjet-based 3D printing process. Knowledge of all of the material factors (such as porosity) that influence the functional properties of the printed devices are needed provide a predictable and reproducible fabrication process.

Conclusions

While the current samples are of low volume fractions of magnetic nanoparticles, this effort demonstrates progress in fabricating 3D functional magnetic composites with arbitrary spatial control of properties that is uniquely possible with inkjet printing techniques. Work is ongoing and improvements in ink formulation and printing protocols can be expected to yield composites with greater magnetic particle content and thereby enhanced magnetic properties, enabling metamaterials with application opportunities in microwave antenna substrates and lenses. Efforts will continue to quantify and refine the process to enable more accurate modeling. Understanding the accuracy, repeatability and maximum magnetic properties achievable by this process is key to understanding how this print technology will ultimately be most useful.

References

[1] K. Alberi, "The 2019 Materials by Design Roadmap," Journal of Physics D: Applied Physics, 52, 1 (2019).

[2] B. Derby, "Inkjet Printing of Functional and Structural Materials: Fluid Property Requirements, Feature Stability, and Resolution," Annual Review of Materials Research. 40, 1 (2010)

[3] S. Ganguly, "Polymer Nanocomposites for Electromagnetic Interference Shielding: A Review," Journal of Nanoscience and Nanotechnology. 18, 11 (2018).

[4] Sushant Agarwal, Rakesh Gupta, Polymer Nanocomposites Handbook. (CRC Press, Boca Raton, FL, 2009), pg. 385–389.

[5] Fengge Gao, Advances in Polymer Nanocomposites : Types and Applications (Elsevier Science & Technology, 2012), pg. 567– 568.

[6] K. Masood, Design and Digital Fabrication of Magneto-dielectric Composites for Additive Manufacturing of Gradient Index RF Lenses. NIP & Digital Fabrication Conference, pg. 94–99. (2019).

[7] Ben Redwood, Filemon Schöffer, Brian Garret, The 3D Printing Handbook: Technologies, Design and Applications (1st ed. 3D Hubs B.V., 2017).

[8] HP Inc., "HP Multi Jet Fusion Technology: Technical White Paper," (2018). [Online]. Available: https://www8.hp.com/us/en/printers/3d-printers/products/multi-jet-technology.html.

[9] M. Vaseem, "Iron Oxide Nanoparticle-Based Magnetic Ink Development for Fully Printed Tunable Radio-Frequency Devices," Advanced Materials Technologies. 3, 4 (2018).

[10] Y. Kim, "Printing Ferromagnetic Domains for Untethered Fast-transforming Soft Materials," Nature, 558, 7709 (2018).

[11] T. N. Do,"Miniature Soft Electromagnetic Actuators for Robotic Applications," Advanced Functional Materials. 28, 18 (2018).

[12] S. Kalia, "Magnetic Polymer Nanocomposites for Environmental and Biomedical applications," Colloid Polymer Science, 292, 9 (2014).

[13] R. De Santis, "3D Fibre Deposition and Stereolithography Techniques for the Design of Multifunctional Nanocomposite Magnetic Scaffolds," Journal of Materials Science: Materials in Medicine. 26, 10 (2015).

[14] F. Ghaffar, "Design and Fabrication of a Frequency and Polarization Reconfigurable Microwave Antenna on a Printed Partially Magnetized Ferrite Substrate," IEEE Transactions on Antennas and Propagation. 66, 9 (20180.

[15] M. Le Floc', "A Physical Model for Heterogeneous Magnetic Materials," Journal of Magnetism and Magnetic Materials. 140 (1995).

[16] R. Ramprasad, "Fundamental Limits of Soft Magnetic Particle Composites for High Frequency Applications," Physica Status Solidi b. 233, 1 (2002)

[17] K. J. Donovan, "Microfluidic Investigations of Capillary Flow and Surface Phenomena in Porous Polymeric Media for 3D Printing," (2019).

[18] Iron Oxide Fe_3O_4 Nanopowder / Nanoparticles (Fe_3O_4, 98+%, 20-30 nm). US Research Nanomaterials, Inc. https://www.us-nano.com/inc/sdetail/234.

[19] L. Preserve, "Magnetite (Fe_3O_4): Properties, Synthesis, and Applications." http://preserve.lehigh.edu/cas-lehighreview-vol-15http://preserve.lehigh.edu/cas-lehighreview-vol-15/5.

[20] Polyamide 12 - Nylon 12 - PA 12 Flexible. AZO Materials. https://www.azom.com/article.aspx?ArticleID=882

[21] Quantum Design, "AC Susceptibility (ACMS II) Brochure" [Online]. Available: https://www.qdusa.com/siteDocs/productBrochures/1084-500_PPMS_ACMS_II.pdf

[22] V. G. Harris, “Modern Microwave Ferrites,” IEEE Transactions on Magnetics, 48, 3 (2012).
[23] R. Samad, “Magneto-dielectric Studies on Multiferroic Composites of Pr Doped $CoFe_2O_4$ and Yb doped $PbZrTiO_3$,” Journal of Alloys and Compounds, 744 (2018).
[24] H. Rocha, “Radio-frequency (RF) Studies of the Magneto-Dielectric Composites: $Cr_{0.75}Fe_{1.25}O_3$ (CRFO)-$Fe_{0.5}Cu_{0.75}Ti_{0.75}O_3$ (FCTO),” Physica B: Condensed Matter, 403, 17 (2008).
[25] Y. Bai, “Magneto-dielectric and Magnetoelectric Anisotropies of $CoFe_2O4/Bi_5Ti_3FeO_{15}$ Bilayer Composite Heterostructural Films,” RSC Advances, 6, 57 (2016).
[26] Ari Sihvola, Electromagnetic Mixing Formulas and Applications (1st ed. The Institution of Electrical Engineers, London, United Kingdom, 1999).

Acknowledgments

This work was supported in part by the National Science Foundation (award no. 1611601).

Author Biography

Madeleine Cannamela received her BS in chemistry from the College of Idaho (2010). She is currently seeking her master’s degree in materials science at Oregon State University, while interning at HP Inc. Her work has focused on 3D printing and voxel doping to create functional materials.

Jim Stasiak is a Distinguished Technologist in HP Labs 3D Printing Laboratory. His research is focused on designing and developing functional polymer nanocomposite materials using 3D printing methods. He is a Fellow of the Society of Imaging Science and Technology (IS&T).

Pallavi Dhagat holds a doctoral degree in Electrical Engineering from Washington University in St. Louis. Currently, she heads the Applied Magnetics Laboratory at Oregon State University and holds a Full Professor position in the School of Electrical Engineering and Computer Science and the Materials Science Graduate Program. She is also the President of the IEEE Magnetics Society and an Adjunct Professor in the Department of Electrical Engineering at the Indian Institute of Technology, Madras.